A. Rydelek and I. S. Sacks, *Geophys. J. Int.* **100**, 39 (1990); L. Seeber and J. G. Armbruster, *Geophys. Res. Lett.* **17**, 1425 (1990); A. J. Michael, W. L. Ellsworth, D. O. Oppenheimer, *ibid.*, p. 1441; A. J. Michael, *J. Geophys. Res.* **96**, 6303 (1991).
5. L. Erickson, thesis, Stanford University (1986).
6. M. Lisowski, W. H. Prescott, J. C. Savage, M. J. Johnston, *Geophys. Res. Lett.* **17**, 1437 (1990). The model dislocation strikes at N44W, dips 70SW, extends 37 km horizontally, has its top at a depth of 5 km and its bottom at a depth of 17.5 km. Right-lateral slip of 1.66 m and reverse slip of 1.19 m yield a moment of 3.0×10^{19} N · m for this model. More complex models of the rupture were also used to predict the static stress changes. Although the results with these models vary in their details, our overall result is apparently not sensitive to the choice of rupture model.
7. See, for example, G. Beroza, *Bull. Seismol. Soc. Am.* **81**, 1603 (1991).
8. In addition, two nonvertical fault segments (198 and 199) were included, representing dipping thrust planes northeast of the San Andreas fault near Los Gatos. A third dipping plane (200) adjacent to the San Gregorio fault was not used in the statistical evaluation, but was added for illustrative purposes [see (*23*)].
9. The depth of the segment centers (6.5 km) coincides with the median depth of seismicity used in this study.
10. J. D. Byerlee, *Pure Appl. Geophys.* **116**, 615 (1978).
11. J. C. Jaeger and N. G. W. Cook, *Fundamentals of Rock Mechanics* (Chapman and Hall, ed. 3, London, 1979).
12. D. H. Oppenheimer, P. A. Reasenberg, R. W. Simpson, *J. Geophys. Res.* **93**, 9007 (1988).
13. For the two dipping fault segments (198 and 199) representing reverse faults, ΔCFF was calculated for the assumption that the dominant shear stress on these planes before the Loma Prieta earthquake was oriented up-dip in a thrust sense.
14. The ranges in these estimates reflect the range in distance of the segments from the Loma Prieta earthquake and uncertainty about rates of loading and magnitudes of earlier earthquakes on these fault segments. No evidence currently justifies estimating the time of advance or delay of the next large earthquake from the modeled average static stress change on a fault. The earthquake process and crustal structure are complex, and the existence of a simple relation between stress change and time to the next large earthquake is as yet unproved.
15. M. V. Matthews and P. A. Reasenberg, *Pure Appl. Geophys.* **126**, 357 (1988). The rate change index β is defined with respect to the null hypothesis, which states that the earthquake occurrence has a Poissonian distribution with the postseismic rate equal to the background rate.
16. The variance was represented by that of a binomial process: $var(n_a) = n_b t_a$.
17. We used $M \geq 1.5$ earthquakes in the U.S. Geological Survey central California catalog.
18. The period 1979 to 1989 produced an unusually large number of ($M \geq 5$) earthquakes in central California, including the 1979 Coyote Lake (M = 5.9), 1980 Livermore (M = 5.9), 1983 Coalinga (M = 6.7), 1984 Morgan Hill (M = 6.2), 1985 Kettleman Hills (M = 5.5), 1986 Mount Lewis (M = 5.7), 1986 Quien Sabe (M = 5.7), 1986 Alum Rock (M = 5.3), and the 1988 and 1989 Lake Elsman (M = 5.0, M = 5.2) earthquakes. This series of earthquakes has been interpreted as possible evidence of an intermediate-term precursory process leading to the Loma Prieta earthquake [L. R. Sykes and S. C. Jaume, *Nature* **348**, 595 (1990)].
19. The background periods 17 October 1969 to 17 October 1979 and 17 October 1969 to 17 October 1989 were also tried, and similar results were obtained. Because of improved stability of the network, the background period 1979 to 1989 is considered most reliable.
20. Significance levels for $|\beta|$ estimated from its asymptotic (Gaussian) distribution are 1.96 (p = 0.05) and 2.57 (p = 0.01).
21. P. A. Reasenberg, *J. Geophys. Res.* **90**, 5479 (1985). Results presented in this paper are based on analysis of the catalog with aftershocks removed. Removal of aftershocks reduced (but did not completely eliminate) these artifacts. The low apparent postseismic rate ($-3 \leq \beta < 0$) remaining in some of these areas (for example, along the Calaveras and Mount Lewis faults) still hampers interpretation of these features as postseismic effects.
22. Apparent changes in seismicity rate may result from man-made factors, including changes in network operations and method used to calculate earthquake magnitude. R. E. Habermann and M. S. Craig [*Bull. Seismol. Soc. Am.* **78**, 1225 (1988)] suggested the presence of such shifts in the catalog during the 1970s. However, because the period 1984 to 1991 is believed to be free of such effects [D. Oppenheimer, personal communication], we do not believe that the seismicity changes we observed are significantly affected by such artifacts.
23. Segments 129, 130, and 131 experienced sizable seismicity rate increases and calculated decreases in $CFF(\mu)$ for all values of friction (see Fig. 3). However, as illustrated by the dipping segment (200) adjacent to segment 130, thrust mechanisms would be favored in this vicinity. Furthermore, earthquake focal mechanism solutions suggest that a majority of the earthquakes there were oblique right-lateral thrust events on dipping planes.
24. We used values of β obtained with aftershocks removed for the background period 1979 to 1989.
25. Evaluation of a fourfold table with a two-sided χ^2 test was carried out on 141 segments. Significance levels for χ^2 are 3.84 (p = 0.05), 6.64 (p = 0.01) and 10.83 (p = 0.001) [see, for example, L. Sachs, *Applied Statistics* (Springer-Verlag, New York, 1982), pp. 346–351].
26. Many of the points in Fig. 3 indicate absolute changes in stress or seismicity on individual segments comparable to the uncertainties associated with modeling errors (stress) and stochastic variance (seismicity). When these tests were applied to a subset of fault segments with significant changes in stress and seismicity (numbered points in Fig. 3), similar results were obtained. χ^2: $p < 0.01$ for $0.1 \leq \mu \leq 0.4$; correlation: ρ exceeds 0.5 for $0.0 \leq \mu \leq 0.3$.
27. T. H. Heaton, *Bull. Seismol. Soc. Am.* **72**, 2181 (1982); M. McNutt and T. H. Heaton, *Calif. Geol.* **34**, 12 (1981); F. D. Stacey, *Physics of the Earth* (Wiley, ed. 2, New York, 1977).
28. E. A. Roeloffs, *J. Geophys. Res.* **93**, 2107 (1988).
29. Using μ = 0.2 we calculated χ^2 for subsets of segments in various ranges of distance from the center of the earthquake dislocation. χ^2 is maximum ($\chi^2 > 21$) for the 80 segments between 0 and 100 km from the source; χ^2 just fails to exceed the p = 0.05 critical point for the farthest 70 segments located 80 or more km from the earthquake.
30. See, for example, J. D. Byerlee and W. F. Brace, *J. Geophys. Res.* **73**, 6031 (1968) and J. H. Dieterich, in *Mechanical Behavior of Crustal Rocks*, N. Carter, M. Friedman, J. Logan, D. Stearns, Eds. (American Geophysical Union, Washington, DC, 1981), pp. 103–120.
31. M. D. Zoback *et al.*, *Science* **238**, 1105 (1987), and references therein.
32. A. H. Lachenbruch and A. McGarr, *U.S. Geol. Surv. Prof. Pap.* **1515**, 261 (1990).
33. For discussions of pore pressure effects see, for example, J. Byerlee, *Geophys. Res. Lett.* **17**, 2109 (1990); J. R. Rice, in *Fault Mechanics and Transport Properties of Rock*, B. Evans and T.-F. Wong, Eds. (Academic Press, London, in press).
34. M. F. Linker and J. R. Rice, *Eos* **72**, 310 (1991).
35. The presence of a buried thrust under the Mission fault was suggested by D. J. Andrews, *Eos* **72**, 446 (1991). Also see R. S. Stein and G. C. P. King, *Science* **224**, 869 (1984); D. L. Jones, A. J. H. Lomax, T. V. McEvilly, *Eos* **72**, 446 (1991).
36. W. L. Ellsworth, J. A. Olson, L. N. Shijo, S. M. Marks, *Calif. Div. Mines Geol., Spec. Publ. 62* (1982).
37. We thank R. Archuleta, W. Ellsworth, A. Lindh, M. Linker, A. Michael, D. Oppenheimer, J. Rice, and P. Segall for helpful discussion and comments and thoughtful reviews of the manuscript.

22 November 1991; accepted 3 February 1992

The Fossil Record and Evolution: Comparing Cladistic and Paleontologic Evidence for Vertebrate History

MARK A. NORELL AND MICHAEL J. NOVACEK

The fossil record offers the only direct evidence of extinct life and thus has figured prominently in considerations of evolutionary patterns. But the incomplete nature of the fossil record has also been emphasized in arguments that fossils play only a secondary role in the recovery of phylogenetic histories based on extant taxa. Although these criticisms recently have been countered, there is no general understanding of the correspondence between the fossil record and phylogeny. An empirical survey of recently published studies suggests no basis for assuming that the stratigraphic occurrence of fossils always provides a precise reflection of phylogeny. Nevertheless, our survey of a sample of taxa shows a tendency for positive correlation between age and clade rank and, hence, a degree of correspondence between phylogenetic pattern and the paleontologic record.

SINCE THE BIRTH OF PALEONTOLOGY the fossil record has been interpreted as a record of life's history. The paleontologic record of horses, for example, has been claimed to demonstrate the potential of fossils in disclosing the branching sequence of taxa through time as well as indicating major evolutionary trends toward increasing specializations (*1–3*). However, what patterns do this record reflect and how precisely do they capture evolutionary events? For instance, fossils have been considered to provide so little evidence for relationships among living taxa that it has been suggested that they be relegated to a secondary role in reconstruction of phylogeny (*4–6*). Such criticisms and recommendations are countered in a recent demonstration that fossil taxa preserve pivotal evidence for ancient

Department of Vertebrate Paleontology, American Museum of Natural History, New York, NY 10024.

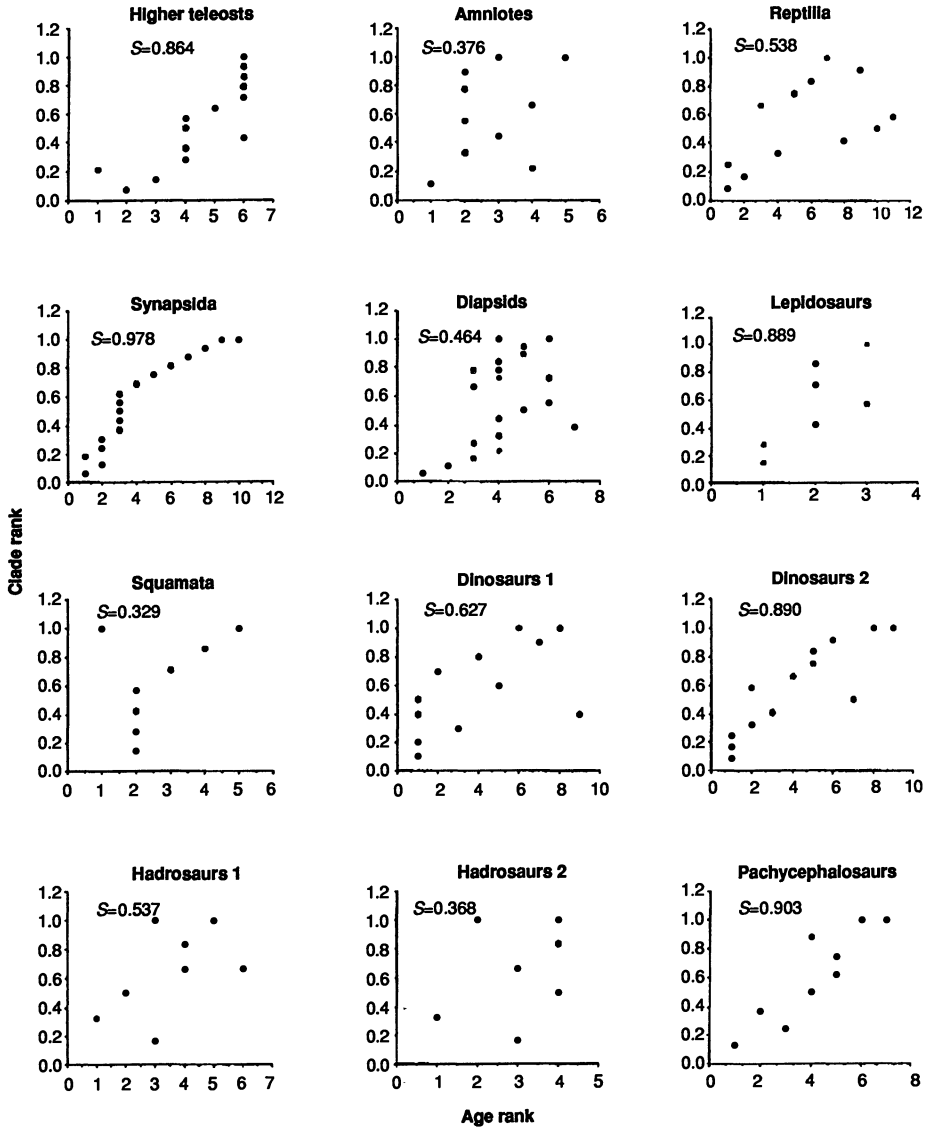

Fig. 1. Plots of age ranks as a function of clade ranks for 12 case studies of fishes and nonmammalian amniote groups. Clade ranks are rescaled from 0 to 1. Correlations are statistically significant (S, Spearman rank correlation coefficient) at $P < 0.01$ for higher teleosts (*8*), Synapsida (7), lepidosaur (*11*), dinosaurs 2 (*13*), and pachycephalosaurs (*15*), and at $P < 0.05$ for Reptilia (7), diapsids (*10*), and dinosaurs 1 (*13*). Correlations are not statistically significant at these levels for amniotes (*9*), Squamata (*12*), hadrosaurs 1 (*14*), and hadrosaurs 2 (*14*).

divergence events among higher amniotes and that the sequence of appearance of fossil amniote taxa closely matches the branching sequence predicted by independent cladistic analysis (7). If this were found to be a general pattern, it would vindicate fossils as a source of phylogenetic information; however, no broader scale examination of empirical cases has been accomplished.

Cladistic analyses of selected vertebrate taxa were compared against the fossil records for those groups (Figs. 1 and 2). Plots were based on studies of higher teleosts (*8*), higher amniotes (*9*), reptiles (7), synapsids (7), diapsids (*10*), lepidosaurs (*11*), squamates (*12*), dinosaurs (*13*), hadrosaurs (*14*), pachycephalosaurs (*15*), higher mammals (*16*), primates (*17*), rodents (*18*), higher ungulates (*19*), artiodactyls (*20*), ruminant artiodactyls (*21*), elephantiformes (*22*), brontotheres (*23*), tapiroids (*24*), chalicotheres (*25*), and equids (*26*). Our purpose was to examine the reliability of the fossil record in recovering the sequence of phylogenetic divergence events. The cladistic result is not necessarily the closer match to the "true" phylogeny; it simply provides an independent means of assessing the timing of evolutionary events in the fossil record. Moreover we assume that the cladistic analyses were developed independent of stratigraphic relationships, although we acknowledge that such stratigraphic information may have played an implicit role in some character analyses. Our comparisons emphasized mammals and other amniotes, where cladistic and age data are most abundant.

We constructed bivariate plots of age ranks against clade ranks as modified from a procedure described by Gauthier *et al.* (7). Clade ranks were assigned with reference to the base of the cladogram; that is, the taxon branching from the basal node was assigned a rank of 1, from the second node from the base, a rank of 2, and so forth (Fig. 3). Taxa branching from the same node were assigned equal clade ranks. Age ranks were derived from the first known occurrence of the taxon in the fossil record. In most cases, age data were given as geologic time intervals (for example, Early Eocene, Wasatchian Land Mammal Age, Late Cretaceous, and so on), but in some cases [such as for horses (*26*)] ages of first occurrence are radiometric dates.

A departure from methods applied elsewhere (7) allows a problem in rank redundancy to be addressed. If a cladogram has several diverging branches each with several subbranches, two or more taxa can be of equal clade rank but have different age ranks based on first occurrence. Each of the branches encompassing these taxa might show a high internal consistency between clade and age ranks but still contribute to the illusion of a weak correlation overall. Such a result could be an artifact of a topology that causes a redundancy in clade ranks rather than a discrepancy between the fossil record and the cladistic branching sequence. For this reason, age ranks against clade ranks were plotted only for those taxa branching from a single spine of the cladogram in a pectinate fashion. All taxa branching from a particular node along this spine were included. Through culling of taxa, side branches were reduced to a single group whose age was indicated by the oldest member of the original side branch. Where data allowed, two or more pectinate components (for example, dinosaurs 1 and 2 in Fig. 1) of a cladogram were analyzed as separate cases.

Age ranks and clade ranks plotted and analyzed for association (Figs. 1 and 2) show variable effectiveness of the fossil record to reproduce a cladistic sequence. Complete congruence between the fossil record and the cladogram in sequence of ranks and level of precision will produce a diagonal line of points intersecting the axes at their origin. Correlations range from poor [higher primates (*17*), higher amniotes (*9*), squamata (*12*), hadrosaurs 2 (*14*)] to high [synapsids (7), pachycephalosaurs (*15*), elephantiformes (*22*), brontotheres (*23*), chalicotheres (*25*), and equids (*26*)]. In some cases, correlations were significant at $P < 0.05$ [(Tapiroids (*24*)] but not compelling (Figs. 1 and 2); rank correlations may be statistically significant but still show considerable deviation of points from a particular trend.

Several aspects of these comparisons are noteworthy. Correlations were diminished where ages were discriminated and cladogram resolution was poor. Thus certain taxa [for example, of higher mammals (*16*), dinosaurs 1 (*13*)] that are part of a polytomous branching pattern, but are known from different ages, are aligned parallel to the abscissa. A converse relationship, however, was more pervasive—namely, one wherein several clades were aligned parallel to the ordinate defined by clade rank. This alignment was expressed in 14 of the cases and was apparent in virtually all the cases, implying a greater potential for resolution through cladistic analysis than through first appearances in the fossil record.

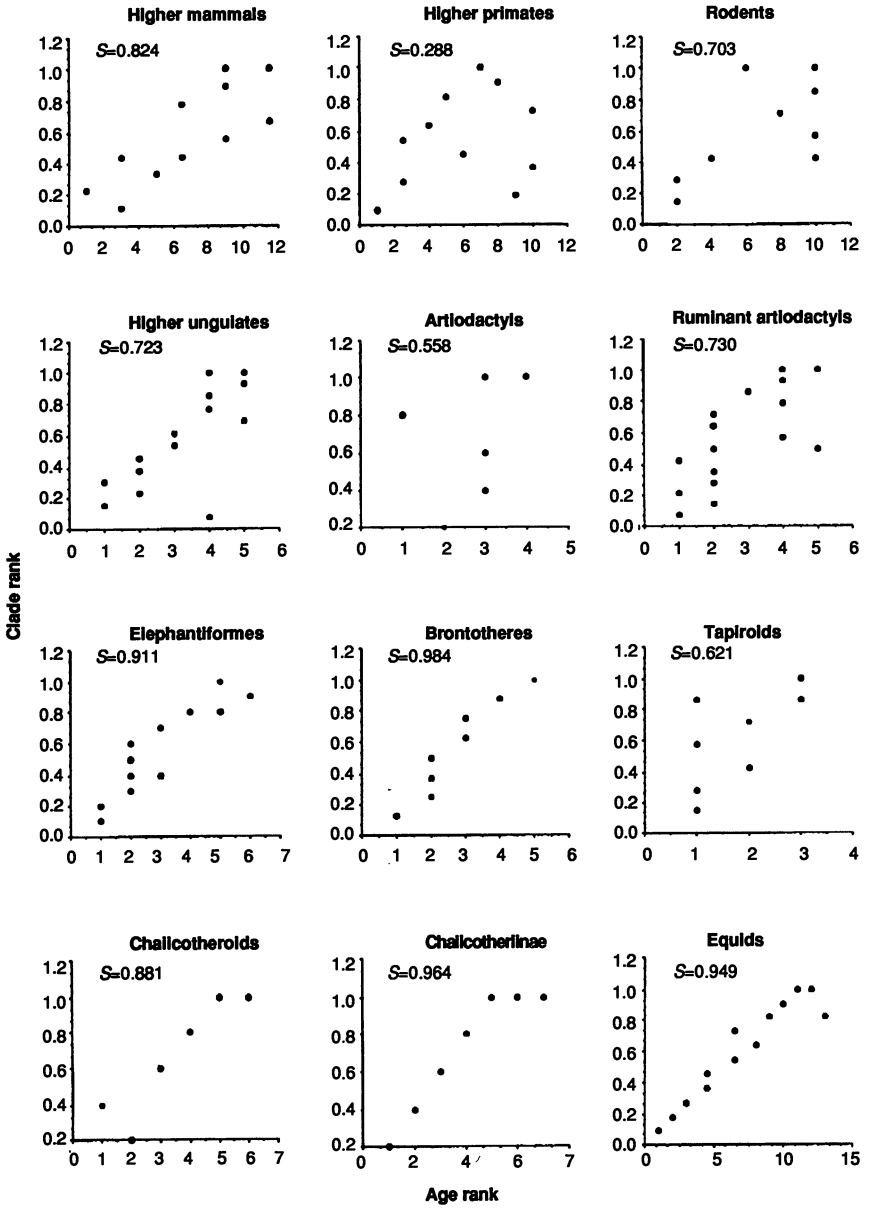

Fig. 2. Plots of age ranks as a function of clade ranks for 12 case studies of mammals as explained in Fig. 1. Spearman rank correlations are statistically significant at $P < 0.01$ for higher mammals (*16*), higher ungulates (*19*), ruminant artiodactyls (*21*), elephantiformes (*22*), brontotheres (*23*), Chalicotheriinae (*25*), and equids (*26*), and at $P < 0.05$ for rodents (*18*), tapiroids (*24*), and chalicotheroids (*25*). Correlations are not statistically significant at these levels for higher primates (*17*) and artiodactyls (*20*).

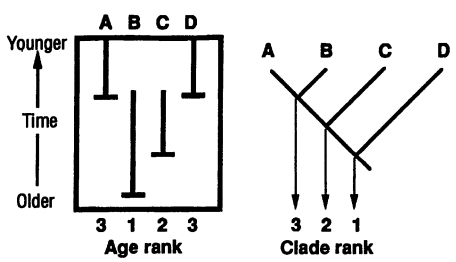

Fig. 3. Age rank and clade rank are determined from fossil records (left) and cladistic phylogenies (right). The fossil record shows the stratigraphic distribution of four taxa. The oldest taxon (B) has an age rank of 1. Taxa A and D appear at the same time; hence, they have equal age ranks. The cladogram (right) shows the phylogenetic relationships of these four taxa. Clade ranks are determined by order of branching from the base of the main cladogram axis.

Correlations are diminished by poor resolution in either age dates or cladograms, and by marked discrepancies between these two sources. For example, the equid (*26*) result shows a clade occurring later in the fossil record than expected from its cladistic position (Fig. 2). Such discrepancies are widespread in certain cases [higher primates (*17*), amniotes (*9*), hadrosaurs 2 (*14*)], and correlations are accordingly poor. Compounding sampling problems are age-scaling factors. More recent fossil records are more finely scaled for age occurrence, placing a high expectation on the consistency between age ranks and clade ranks. Conversely, age dates for groups with long fossil histories seem more robust. If intervals between age ranks are more extensive, ages of first occurrence may be inaccurate by tens of millions of years without modifying age rankings. Such a pattern may pertain to the synapsid record (Fig. 1).

The relationships examined here also reveal that the quality of the fossil record judged from other perspectives does not necessarily predict its match with independently derived phylogenetic evidence. The documented fossil record of primates is generally regarded as one of comparatively high quality based on the diversity and widespread geographic and geochronologic distribution of primate fossils and the amount of attention the group has received (*27*). Yet the primate fossil record poorly reflects higher level cladistic branching patterns (*17*). This is because some taxa (tarsiers and cheirogalines, for instance) thought to have branched off very early in primate history appear late in the record or have no fossil record (Fig. 2).

Despite these discrepancies, there is a noteworthy correspondence between the fossil record and the independently constructed phylogeny for many vertebrate groups. Statistically significant correlations ($P < 0.05$) were found in 18 of the 24 cases examined. Correspondence is particularly evident in some of the mammalian ungulate groups. For example, the impression that the fossil record of horses provides an excellent picture of the history of this group is extended to the remarkable match of that record with cladistic results.

REFERENCES AND NOTES

1. W. D. Matthew, *Q. Rev. Biol.* **1**, 139 (1924).
2. R. A. Stirton, *Univ. Calif. Publ. Geol. Sci.* **25**, 165 (1940).
3. G. G. Simpson, *Horses* (Oxford Univ. Press, New York, 1951).
4. W. Hennig, *Insect Phylogeny* (Wiley, New York, 1981).

5. C. Patterson, *Annu. Rev. Ecol. Syst.* **12**, 195 (1981).
6. M. Goodman, in *The Hierarchy of Life*, B. Fernholm, K. Bremer, H. Jornvall, Eds. (Elsevier, Amsterdam, 1989), pp. 43–61.
7. J. A. Gauthier, A. G. Kluge, T. Rowe, *Cladistics* **4**, 105 (1988).
8. G. V. Lauder and K. F. Liem, *Bull. Mus. Comp. Zool.* **150**, 95 (1983).
9. J. A. Gauthier, A. G. Kluge, T. Rowe, in *The Phylogeny and Classification of the Tetrapods*, M. J. Benton, Ed. (Clarendon Press, Oxford, 1988), vol. 1, pp. 103–155.
10. S. E. Evans, in (*9*), pp. 221–260.
11. J. A. Gauthier, R. Estes, K. De Queiroz, in *Phylogenetic Relationships of the Lizard Families*, R. Estes and G. Pregill, Eds. (Stanford Univ. Press, Palo Alto, 1988), pp. 15–98.
12. R. Estes, K. De Queiroz, J. A. Gauthier, in (*11*), pp. 119–281.
13. M. J. Benton, in *The Dinosauria*, D. B. Weishample, P. Dodson, H. Osmolska, Eds. (Univ. of California Press, Berkeley, 1990), pp. 11–30.
14. D. B. Weishample and J. R. Horner, in (*13*), pp. 534–561.
15. T. Maryanska, in (*13*), pp. 564–577.
16. M. J. Novacek, in *The Hierarchy of Life*, B. Fernholm, K. Bremer, H. Jornvall, Eds. (Elsevier, Amsterdam, 1989), pp. 421–435.
17. P. Andrews, in (*9*), vol. 2, pp. 143–175.
18. J.-J. Jaeger, in (*9*), vol. 2, pp. 177–199.
19. D. R. Prothero, E. M. Manning, M. Fischer, in (*9*), vol. 2, pp. 201–234.
20. A. Gentry and J. J. Hooker, in (*9*), vol. 2, pp. 235–272.
21. C. Janis and K. Scott, in (*9*), vol. 2, pp. 273–282.
22. P. Tassy and J. Shoshani, in (*9*), vol. 2, pp. 283–315.
23. B. J. Mader, in *The Evolution of Perissodactyls*, D. R. Prothero and R. M. Schoch, Eds. (Clarendon Press, Oxford, 1989), pp. 458–484.
24. R. M. Schoch, in (*23*), pp. 298–320.
25. M. C. Coombs, in (*23*), pp. 438–457.
26. R. L. Evander, in (*23*), pp. 109–126.
27. R. L. Caroll, *Vertebrate Paleontology and Evolution* (Freeman, New York, 1988).
28. We thank G. Naylor, S. Blum, N. Eldredge, W. Wheeler, R. Voss, and J. Gauthier for helpful discussion.

21 October 1991; accepted 16 January 1992

Predisposition to Renal Cell Carcinoma Due to Alteration of a Cancer Susceptibility Gene

CHERYL WALKER, THOMAS L. GOLDSWORTHY, DOUGLAS C. WOLF, JEFFREY EVERITT

A single germ line gene mutation at a tumor susceptibility locus in a rodent model of hereditary human renal cancer caused a 70-fold increase in susceptibility to chemical carcinogenesis. A carcinogen that targeted both renal epithelial and mesenchymal cells caused an increase in tumors of epithelial origin in susceptible animals; the number of carcinogen-induced mesenchymal tumors was unaffected by the presence of the mutation at the susceptibility locus. Thus, this mutation defines a genetic locus for susceptibility to carcinogen-induced tumors and modulation of carcinogen susceptibility by this locus exhibits cell-type specificity.

THE DEVELOPMENT OF GENETIC markers to identify individuals predisposed to tumor development after occupational or environmental exposure to potential carcinogens will require an understanding of how specific genes determine susceptibility for the induction of cancer by chemical carcinogens. Knowledge of the proportion of susceptible individuals in the population and the relative cancer susceptibility of normal and predisposed groups will make it possible to estimate human risk from carcinogen exposure. In addition, it may be possible to limit the exposure of these susceptible individuals to potential carcinogens.

Tumor suppressor genes represent one class of cancer susceptibility genes in humans (*1*). Inheritance of a mutation in one allele of a tumor suppressor gene predisposes individuals to develop tumors after sustaining an additional spontaneous mutation in the remaining normal allele of that gene (*2*). It follows from this work that inheritance of a mutation in a susceptibility gene would also predispose to the induction of tumors by chemical carcinogens.

In human renal cell carcinoma (RCC), loss of heterozygosity of chromosome 3 occurs frequently (*3*), and inheritance of an alteration at this putative tumor suppressor locus in von Hippel–Lindau disease predisposes to the development of RCC (*4*). In rats, a single gene mutation [described by Eker and Mossige (*5*)] predisposes to multiple bilateral RCCs with an autosomal dominant pattern of inheritance, and animals carrying the Eker mutation serve as a model for hereditary RCC (*6*). Rats that are heterozygous for the gene defect develop spontaneous RCCs between 4 and 12 months of age (*7*), whereas rats that are homozygous for the wild-type allele rarely develop spontaneous RCC (<0.5%) (*8*). When homozygous, the mutation is lethal prenatally at 9 to 10 days of gestation (*7, 9*).

The hereditary tumors that develop in the Eker rat model have many similarities to their human counterparts: they have similar histology, are bilateral, overexpress transforming growth factor (TGF-α), and do not exhibit a high frequency of *ras* oncogene activation (*10*). Loss of sequences on rat chromosomes 4 (q11 through qter), 5 (monosomy), and 6 (q24) occur in these tumors and tumor-derived cell lines, suggesting that the location of the susceptibility gene may reside on one of these chromosomes (*11*). Animals carrying the Eker mutation develop hemangiosarcomas in the spleen (males and females) and uterine leiomyosarcomas as second primary tumors later in life (*12*). Vascular neoplasms (hemangioblastomas) and second primary tumors are also associated with RCC in human von Hippel–Lindau disease (*13*).

In rats carrying the Eker mutation, it is possible to test for carcinogen susceptibility (as measured by increased kidney tumor multiplicity) and cell type specificity in two distinct cell populations, renal tubular epithelial cells and renal mesenchymal cells. The carcinogen dimethylnitrosamine (DMN) induces both renal cell adenomas and carcinomas (renal cortical tumors = RCT), arising from tubular epithelial cells, and renal mesenchymal tumors (RMT), arising from stromal cells of the kidney (*14*). F1 offspring of heterozygous rats carrying the Eker mutation (*15*) were exposed to a single carcinogenic dose of DMN (30 mg per kilogram of body weight) at 16 weeks of age (*16*). The mutation segregates as a single-locus autosomal dominant; therefore, one-half to two-thirds of the carrier F1 rats would be expected to carry the Eker mutation. At 12 months of age, tumors were quantitated by light microscopy in each kidney of the carrier F1 rats and in kidneys of a control group of wild-type rats exposed under identical conditions (*16*).

Carrier F1 rats exposed to the chemical carcinogen showed a large increase in tumor number (Table 1 and Fig. 1). The number of spontaneous RCTs ranged from 1 to 14 tumors per animal in the unexposed carrier F1 males. In the DMN-exposed carrier F1 males, more than half had >16 tumors per animal, with one DMN-exposed animal having 90 RCTs. In wild-type males, the same dose of DMN was marginally carcinogenic (Table 1 and Fig. 1). Thus, after the background incidence of spontaneous tumors was subtracted (male F1 offspring of gene carriers developed an average of 2.8 RCTs per animal), a 70-fold increase in tumor susceptibility (23 versus 0.33) could be attributed to the presence of the Eker mutation in the carrier F1 animals (*17*). The combined effect of the mutation and carcinogen exposure was a three to four orders of magnitude increase in tumors relative to the spontaneous tumor frequency in wild-type rats (25.6 versus 0.005).

Chemical Industry Institute of Toxicology, P.O. Box 12137, Research Triangle Park, NC 27709.